Structural Characterization of Multilayered DNA and Polylysine Composite Films: Influence of Ionic Strength of DNA Solutions on the Extent of DNA Incorporation

Xiangyang Shi, Raymond J. Sanedrin, and Feimeng Zhou*

Department of Chemistry and Biochemistry, California State University, Los Angeles, Los Angeles, California 90032

Received: August 24, 2001; In Final Form: November 14, 2001

Thin films of alternating DNA and poly-L-lysine (PLL) layers were fabricated onto various planar surfaces by the layer-by-layer (LbL) self-assembly technique. For both the polydeoxynucleotide (PDN, polyguanylic acid or poly[G]) and the oligodeoxynucleotide (ODN, a 30-mer) investigated, UV−visible spectrometry and contact angle measurements showed that a uniform layer of DNA can be fully adsorbed onto each alternate PLL layer. Various parameters affecting the DNA loading into the composite film were investigated with a particular emphasis placed on the effect of the ionic strength in the DNA solution used for the film preparation. For the PLL/poly[G] film, it was found that 150 μg/mL of poly[G] solution containing 0.5 M NaCl attains the maximum loading for every poly[G] layer. Atomic force microscopy was utilized to measure the DNA surface density and structure at the topmost layers of several representative composite films. While the DNA film thickness increases with the ionic strength of the DNA solution, the shape of the DNA molecules adsorbed through the LbL assembly was found, for the first time, to undergo a transition from extended linear structure to a more circular or coiled configuration. The AFM images, together with results accumulated from the UV−visible spectrometric and quartz crystal microbalance experiments, helped to unravel the relationship between the DNA surface structure/loading and the ionic strength of the DNA solution. Our study clarified a possible misconception about the proportionality between DNA thickness and DNA incorporation/loading. It also provided a fundamental understanding about and the practical guidance for the utilization of the LbL method to construct DNA multilayers or polymer-encapsulated DNA molecules for gene-delivery applications.

1. Introduction

The past few years have seen a rapid advancement in developing effective nonviral drug delivery systems.[1] Some of the key factors affecting the efficacy and safety of a specific gene delivery method include, but are not limited to, the amount of DNA molecules incorporated, the integrity of the DNA structures and functions, the sustainability of the encapsulating layers under various physiological conditions, the low toxicity of the encapsulating materials, and the possibility of controlled release of the encapsulated genes. Along this line, various DNA nanoparticulate systems have been employed for gene delivery applications.[2] DNA can be adsorbed onto cationic polymer[3] or colloidal silica particles[4,5] for nonviral transfection. Recent studies have also shown that chitosan,[6] gelatin,[7] protamine,[8] polymers such as poly(ethylenimine) and polylysine,[9,10] copolymer-DNA nanoparticles[11−14] prepared by coacervation, complexation, phase inversion/solvent diffusion, and solvent evaporation methods, etc. can be used as gene carriers.

The layer-by-layer (LbL) assembly of different components, on a separate front, has shown to be an attractive avenue for fabrication of thin films of ordered structures containing various functional supramolecular moieties.[15] A common approach based on the LbL method is via electrostatic attraction between oppositely charged polyelectrolytes, permitting sequential deposition of these species from diluted solutions onto a surface. Multilayer films of polyelectrolytes,[15] proteins,[16−18] dyes,[19−21] clays,[22−26] and various nanoparticles[27−35] have been constructed. The advantage of the LbL method is that the layer thickness and composition can be precisely tailored by varying the number of adsorption cycles and the type of charged species. There have been some reports about the LbL self-assembly of polydeoxynucleotide (PDN) multilayers as potentially useful DNA sensors.[36−39,40] The growth of DNA multilayers can be confirmed by small-angle X-ray scattering,[37,38] the surface plasmon resonance technique,[41] and UV−visible spectrometry.[42] Several studies, prompted by the need to understand drug−DNA interactions, investigated the intercalation of and recognition for various aromatic compounds by surface-confined DNA molecules.[42−44]

Because of the controllability associated with the LbL method, multilayers of DNA films on colloidal particles could be tailored to become promising gene therapy carriers. Dudnik and coworkers[45] have compared different preparation methods for coating DNA or polymer multilayers onto colloidal melamine formaldehyde core particles. In a recent study, Trubetskoy et al. deposited oppositely charged polyelectrolytes on the surface of condensed DNA particles by the LbL self-assembled technique.[46]

Despite the various developments of polymer−DNA composite films or capsules based on the LbL method, factors affecting the DNA incorporation into the films as a dense package have not been thoroughly studied. Condensing DNA to small sizes is an important prerequisite for developing an advanced gene delivery system because the densely packed DNA molecules can be more easily taken up by cells.[1] Although it has been noted that the thickness of a polycationic film deposited onto a polyanionic film (or vice versa) is dependent

* To whom correspondence should be addressed. Phone: 323 343 2390. Fax: 323 343 6490. E-mail: fzhou@calstatela.edu.

10.1021/jp0132634 CCC: $22.00
Published on Web 01/12/2002

on the ionic strength of the solution,[42] there is a lack of detailed understanding about the interplay between the parameters for film preparations and the resultant DNA film structure and the amount of DNA incorporation. Moreover, it is not clear whether a thicker DNA film would correspond to a greater extent of DNA loading, given the possibility that the DNA adsorption processes might be dependent on solution conditions (e.g., ionic strength and pH).

In this study, multilayers of alternating PDNs or oligodeoxynucleotides (ODNs) and poly-L-lysine (PLL) layers were constructed using the LbL method. Single-stranded polyguanylic acid (5′) (poly[G]) was selected as a representative PDN, whereas a 30-mer ODN was chosen to determine whether the DNA incorporation into the polymer/DNA film is dependent on the size of the DNA. The growth of each PLL and DNA layer was followed by UV−visible spectrometry and contact angle measurements. The structure of the topmost PDN layer was characterized by atomic force microscopy (AFM). Quartz crystal microbalance (QCM) was used to deduce the ratio between the amount of PLL and that of the DNA adlayers. These four independent techniques provide complementary information about the LbL formation of the PLL/DNA composite films. AFM probes the surface structure of the DNA layer at the molecular level in a localized region, whereas the other three techniques study each layer or the entire film at a macroscopic level. While the DNA concentration used and the number of layers produced were both found to alter the amount of DNA incorporation in a predictable way, the dependence of the DNA incorporation (loading) into the multilayered composite films on the ionic strength of the DNA solutions showed a somewhat unexpected behavior. A systematic characterization of the various PLL/poly[G] films formed at different NaCl concentrations (ionic strengths) was therefore performed. The AFM images of the various DNA surface structures provided a possible explanation about our observations.

2. Experimental Section

2.1. Materials. Poly-L-lysine (PLL, MW 37 700) and polyguanylic acid (5′) (poly[G], MW 8000−500 000) were purchased from Sigma. The range of the poly[G] molecular weights is 8000−500 000. Thus, the lengths of poly[G] should be roughly between 7.2 and 447 nm, if 0.34 nm is used as the base spacing.[47] 3-Aminopropyltriethoxysilane (APTES) and mercaptopropionic acid (MPA) were acquired from Aldrich. Sodium chloride was obtained from Fisher. The ODN used contained 30 bases with a sequence of 5′-AGAGGATCCCCGGGTACCGAGCTCGAATTC-3′ (Integrated DNA Technologies, Inc., Coralville, IA). Water used was treated with a Millipore Milli-Q Plus 185 purification system and had resistivity higher than 18.2 MΩ cm.

2.2. Preparation of DNA Multilayer Films. *Quartz Substrates.* Thin, alternating PLL/DNA multilayer films were LbL-assembled onto quartz substrates (Hellma, Germany), cleaned through soaking in a 5:1:1 (vol %) $H_2O/H_2O_2/NH_3$ mixture at 70 °C for 10 min (RCA protocol)[48,49] and rinsed with a copious amount of water. The first layer of PLL was adsorbed onto the quartz surface by immersing the quartz substrate in a 0.5 mg/mL PLL/0.5 M NaCl solution for 15 min. The PLL-covered substrates were then dipped in water three times, followed by drying under a stream of N_2. Poly[G] or the 30-mer ODN was then attached to the PLL layer. Multilayer composite films composed of alternating PLL and DNA layers were formed from DNA solutions of varying NaCl contents. The DNA attachment was monitored by UV−visible spectrometry (SLM-AMINCO, model 3000).

Silicon Wafers and Mica Surfaces. Silicon wafers (111) were treated using the RCA protocol described above. Thin films of PLL/poly[G] multilayers were assembled onto the silicon wafers with the aforementioned procedure. Verification of the PLL and DNA attachments and the extent of coverage of these layers was carried out using a contact angle meter (KSV Instruments, Monroe, CT). Measurements of the contact angles were performed at individual polyelectrolyte layers. All of the reported values are the average of at least five measurements. Freshly cleaved mica sheets, which are suitable for high-quality AFM imaging, were also used as substrates for the sequential PLL and poly[G] adsorption.

QCM Electrodes. AT-cut 9.995 MHz crystals (ICM Technologies, Oklahoma City, OK) with both sides coated with polished gold films were employed for the PLL/poly[G] multilayer formation. The crystal surface was cleaned with a piranha solution (30% H_2O_2 and 70% concentrated H_2SO_4). *CAUTION: Piranha solution reacts violently with organic solvents and is a skin irritant. Extreme caution should be exercised when handling piranha solution.* Frequency measurements were carried out through the use of an ICM oscillator and a PM6680B counter/timer (Fluke Corp., Everett, WA).

The total mass deposited at the QCM crystal surface can be calculated from the cumulative frequency change using the Sauerbrey equation.[50] For a 9.995 MHz QCM crystal with an electrode area of 0.196 cm^2, the relationship between the adsorbed mass (Δm) of each poly[G] and PLL layer and the change in the resonant frequency (ΔF) is given by

$$\Delta m(\text{ng}) = -0.86\Delta F(\text{Hz}) \quad (1)$$

2.3. Atomic Force Microscopy (AFM). AFM measurements were conducted using an atomic force microscope equipped with a magnetic alternating current (MAC) mode (Molecular Imaging, Phoenix, AZ). Both contact and MAC modes were employed for the characterization of PLL/poly[G] multilayer films. The MAC cantilever tips used had a spring constant of 0.5 N/m. Images of multilayer films of PLL/poly[G] on silicon wafers and mica sheets were obtained using an oscillating frequency of 25 kHz and a driver current of 30 ± 5 A. The amplitude change of the probe was sufficiently low, and consequently, the imaging was nondestructive to the samples.[51]

3. Results and Discussion

3.1. Fabrication of Multilayered DNA and Polylysine Films. The LbL assembly of PLL and poly[G] thin films was performed on quartz substrates. The absorption spectrum (Figure 1) is characteristic of the DNA adsorption and agrees well with previously reported absorption spectra.[42] Note that PLL does not show any absorption in the wavelength range shown in Figure 1. Consequently, the plot of absorbance at 260 nm vs the layer number (inset of Figure 1) shows the stepwise increase only at the even number. Lang and Liu have shown that the incremental increase of absorption in the poly(allylamine hydrochloride)/salmon spermary DNA composite film is indicative of a uniform coverage of DNA molecules onto the polyelectrolyte layer.[42] We also investigated the relationship between the amount of DNA loading and the concentration of DNA used for the film preparation. Figure 2 shows the absorbance of the individual PLL/poly[G] bilayers at 260 nm as a function of the poly[G] concentration. As can be seen, all of the PLL/poly[G] bilayers showed a gradual increase in absorbance between 1 and 100 μg/mL. At 150 μg/mL, an abrupt increase in the DNA loading was observed. Further increase in the DNA concentration did not significantly alter the amount

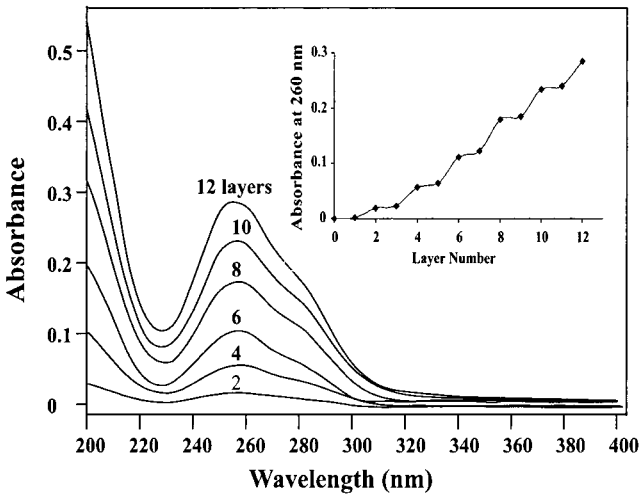

Figure 1. UV−visible absorption spectra of PLL/poly[G] multilayer films assembled on quartz substrates. The DNA solution used for the film preparation contained 150 μg/mL of poly[G] and 0.2 M NaCl. The inset shows a plot of the poly[G] absorption at 260 nm as a function of the layer number. The odd layer numbers correspond to PLL and the even layer numbers to poly[G].

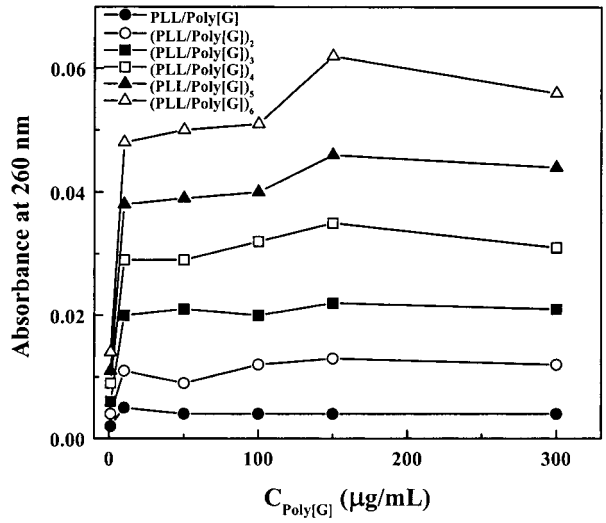

Figure 2. Absorbance values of $(PLL/poly[G])_n$ multilayer films at 260 nm vs poly[G] concentrations employed for the film fabrication.

of DNA incorporated. On the basis of this study, we chose 150 μg/mL as the optimal poly[G] concentration to construct films used for the surface characterization described in the following sections.

We should mention that it is difficult to accurately deduce the amount of DNA adsorption given the possibility that the orientations of chromophores on the surface-confined DNA molecules affect the overall absorbance value. A recent AFM study reported that polyelectrolyte adsorption behavior is dependent on the number of adsorption layers.[52] This suggests that the surface orientations of the polyelectrolyte adsorbates at the outer layers might be different than those of the molecules residing in the inner layers. Thus, the UV−visible spectra are semiquantitative at best and should not be used to calculate the absolute amount of adsorbed DNA molecules.

To further verify the buildup of PLL/poly[G] multilayer films, the contact angle at each polyelectrolyte layer was measured. The contact angle measurement should allow the compactness of each adlayer to be assessed because PLL is known to be more hydrophobic than nucleic acids.[53] The adsorption of the first PLL layer onto silicon wafers resulted in a contact angle

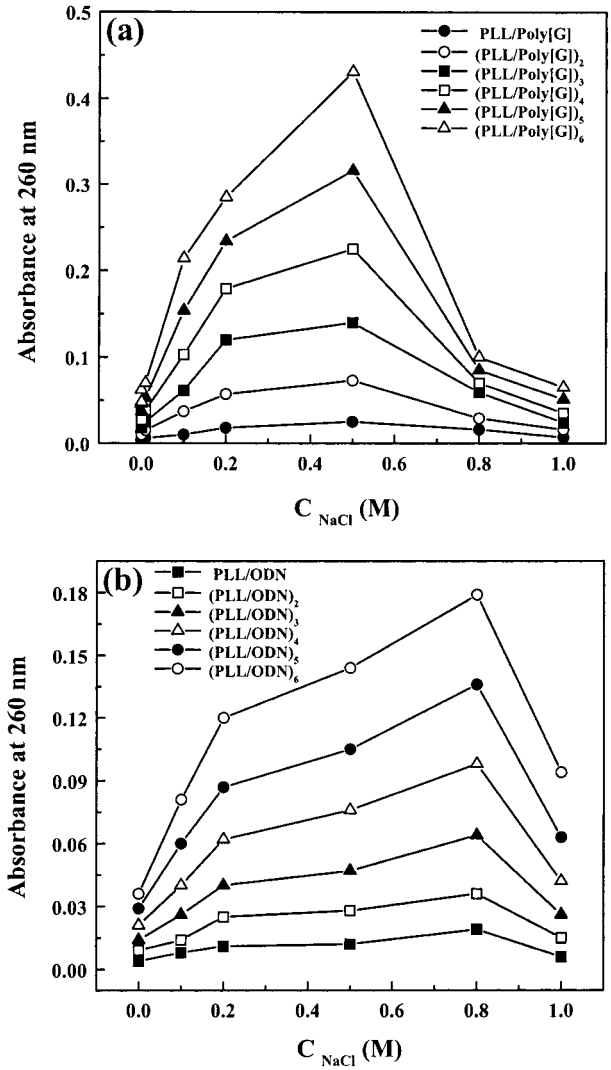

Figure 3. Absorbance values of individual PLL/DNA bilayers in the multilayered films plotted as a function of NaCl concentrations used for the film preparation. Panel a shows the bilayer containing poly[G] formed from 150 μg/mL poly[G] solutions, and panel b depicts the bilayer constituting a 30-base oligodeoxynucleotide constructed using a concentration of 150 μg/mL.

of 23° ± 2°. This value decreased to about 10° ± 1° after the subsequent deposition of poly[G]. Such an obvious change is in line with the difference in the hydrophobicities of PLL and poly[G]. Further alternate depositions of PLL and poly[G] layers caused the contact angle to flip-flop between these two values (data not shown), suggesting that each additional layer of polyelectrolyte fully covered the preceding layer. This observation is consistent with the conclusion drawn from the UV−visible spectrometric experiments.

3.2. Effect of Ionic Strength of the DNA Solution on the DNA Loading. As stated in the Introduction, the objective of this work is centered on the elucidation of the experimental parameters that affect the DNA loading in the PLL/DNA composite films. In addition to the aforementioned investigations on the effect of the DNA concentration and the layer number, we carried out a study to examine the influence of the ionic strength of the DNA solution on the final amount of DNA incorporated into the composite films. Figure 3a is a plot of the absorbance values of $(PLL/poly[G])_n$ multilayer films at 260 nm as a function of the NaCl concentrations in the poly[G] solutions. Because the ionic strength is the same as the formal concentration for a 1:1 electrolyte such as NaCl, ionic strength

and electrolyte concentration are used interchangeably to describe the salt effect for the remainder of the paper. Two points are worth mentioning. First, for all of the poly[G] solutions of different NaCl concentrations, the amount of poly[G] loaded into the film is proportional to the layer number. This trend has also been reflected by the linear increase in absorbance (Figure 1). The second point is related to an interesting observation that we made regarding the correlation of the extent of DNA incorporation with the ionic strength of the DNA solution. As shown in Figure 3a, when the NaCl concentration was about 0.5 M, the poly[G] loading reached a maximum value. Too little (e.g., 0−0.1 M) or too much (e.g., 1.0 M) NaCl in the poly[G] solutions would not yield a high poly[G] incorporation, suggesting that the ionic strength of the DNA solution has a profound influence on the ultimate quantities of DNA anchored onto the PLL layers. We found that this trend is not unique to PDNs such as poly[G] because the LbL assembly of PLL and an ODN of 30 bases also displayed a similar dependence on the electrolyte concentration of the DNA solution. Curves shown in Figure 3b all exhibit an absorption maximum in the same NaCl concentration range studied, though the position of the maximum shifted to a slightly higher NaCl concentration (∼0.8 M). Thus far, the observation of such a dependency has not been reported and elaborated. We think that, given that the conformation or structure of both ODNs and PDNs are known to be related to the ionic strength of the solution,[54] the electrolyte content of the DNA solution should play an important role in the degree of DNA condensation onto the PLL layer. At low NaCl concentrations, the DNA strands are more stretched because the multiple negative charges on the phosphate groups residing on the DNA chain tend to repel each other. As the concentration of the NaCl increases, the countercations (Na^+ in the present case) would help alleviate the Coulombic repulsion among the phosphate groups, and consequently, the DNA strands might be more coiled up or intertwined together. The less-extended DNA structure would facilitate the packaging of a greater number of DNA molecules in a given surface area. Therefore, the surface density of DNA molecules (or the thickness of the DNA layer) on top of the PLL layer would increase. The precipitous decline in the DNA loading at a NaCl concentration greater than certain values (0.5 M for poly[G] and 0.8 M for the 30-mer) can be interpreted as follows. As the ionic strength of the DNA solution becomes quite high, cations in the solution can effectively shield the phosphate groups on the DNA strands from the lysine groups of the PLL layer. As a result, the electrostatic attraction that is essential to the LbL assembly of the DNA/polymer composite film is no longer operative. The consequence of the weakened electrostatic attraction appears to more than offset the extensively coiled DNA structures for favoring a dense packing of DNA molecules onto the preceding PLL layer. The AFM images and the QCM results described below provide evidences purporting the above reasoning.

We should note that the above interpretation is based on a simplistic approach, which does not take into account the polarizability of the ionic groups present in the DNA molecules and the details of DNA structures (which are much more complex and flexible than that of rigid polyelectrolytes).

3.3. Structural Characterization and Quantification of PLL/Poly[G] Multilayers Formed at Different Ionic Strengths. To corroborate the relationship between the extent of DNA loading and the DNA structure in films made at different ionic strengths, we used AFM to determine the surface density and structure of the DNA molecules. Figure 4a−d presents the AFM images of $(PLL/poly[G])_3$ films assembled in poly[G] solutions containing 0, 0.1, 0.5, and 1.0 M NaCl, respectively. These films clearly show a gradual variation of the DNA structure and surface density. In the absence of NaCl, stretched poly[G] strands can be resolved (e.g., the molecule of which the ends are indicated by the arrows in Figure 4a). Strands of different lengths can be found in this image, with most of them between 110 and 185 nm (Table 1). This range is well within that deduced based on the molecular weight distribution of the poly[G] molecules (7.2 and 447 nm). The average height of most of the DNA strands, deduced from the cross-sectional contours in Figure 4a, is 2.1 ± 0.2 nm. Previously, Sukhorukov et al. measured the average thickness of a PLL/polyuridylic acid bilayer to be 2.5 ± 0.5 nm using X-ray reflection.[38] Thus, the height of the DNA strands determined by our AFM is reasonable. Such a value is also consistent with the width of a double-stranded DNA molecule.[47] Both the height and length values suggest that most of the rambling poly[G] strands are lying flat on the PLL layer. Moreover, given the fact that both our results and the X-ray reflection[38] yielded heights not much greater than 2.0 nm, it is clear that only one layer of DNA resides on top of the PLL layer. The width of a typical DNA strand (Table 1) is comparable to that of extended calf thymus DNA molecules immobilized onto self-assembled alkanethiol films.[51] The wider-than-expected strand width has been attributed by us[51] and other researchers[55,56] to the image-broadening effect caused by the interaction between the AFM tip and the flexible DNA molecules. The many void spaces in Figure 4a qualitatively indicate the incompactness of the poly[G] layer.

When the electrolyte concentration was increased to 0.1 M, somewhat coiled poly[G] molecules were found to disperse onto the PLL layer (Figure 4b). The cross-sectional contours of Figure 4, parts a and b, display a difference in the thickness/height of the topmost poly[G] layer (see Table 1), confirming that the DNA film has become thicker in the presence of 0.1 M NaCl. Note that the shape of the DNA molecules is more circular (diameters of most circles are 50−60 nm), suggesting that the DNA strands have been folded into coiled configurations. These coiled structures should allow a greater number of DNA molecules to pack onto the PLL layers. The extent of the poly[G] folding at a greater ionic strength is expected to be even more pronounced. This folding resulted in a greater DNA surface density (compare the surface densities shown in Table 1). The surface density was further increased at a typical film shown in Figure 4c (also see Table 1), which was prepared using a 0.5 M NaCl solution. The cross-sectional contour of Figure 4c also confirms that the poly[G] molecules have become rounder (with the diameters increased to a range between 75 and 100 nm). The average height of poly[G] molecules was augmented to 8 ± 0.7 nm. Clearly, the diameter of these spherical features is less than the length of the strands in Figure 4a, suggesting again that the long strands of DNA have been twined into the coiled structures when 0.5 M NaCl was used.

The AFM image of a $(PLL/poly[G])_3$ film fabricated with a 150 μg/mL poly[G]/1.0 M NaCl solution is given in Figure 4d. Compared to Figure 4 parts b and c, the poly[G] molecules have become even bulkier and more oblong (see Table 1 for the average height and length), but the packing of these DNA molecules is much scarcer. The poly[G] surface density (1.5×10^{14} molecules/cm^2) is smaller than that of the films prepared with 0.1 and 0.5 M NaCl.

We should caution that, in deducing the poly[G] surface density, we did not consider the possible tangling of several poly[G] molecules to form one circular feature. Consequently,

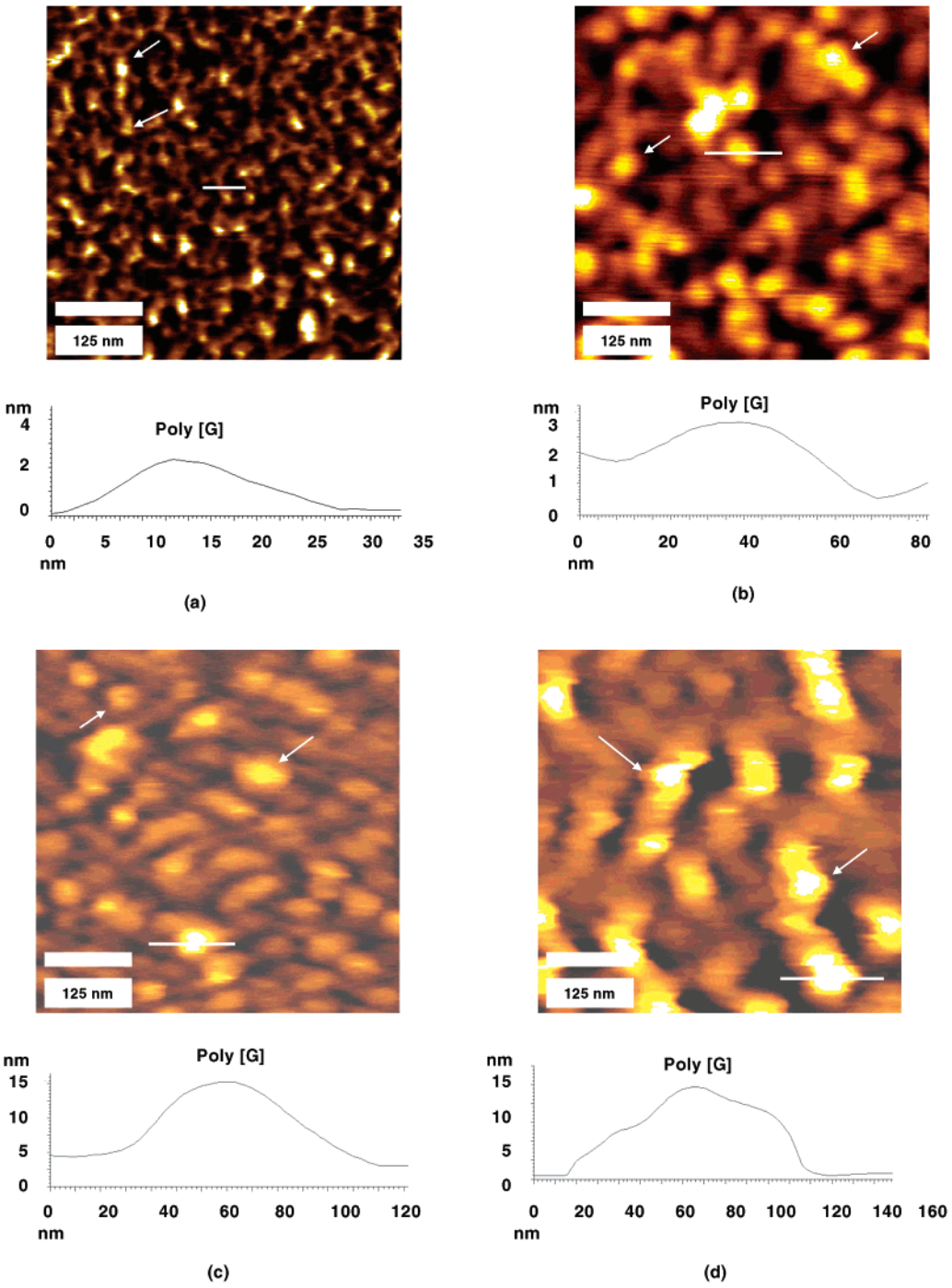

Figure 4. Topographical AFM images of $(PLL/poly[G])_3$ assembled using 150 μg/mL poly[G] solutions containing (a) 0, (b) 0.1, (c) 0.5, and (d) 1 M NaCl. The two arrows in panel a show the ends of a stretched poly[G] molecule, and arrows in other images indicate individual poly[G] molecules. The cross-sectional contour of each image is also provided.

the surface densities listed in Table 1 for Figure 4b−d might be underestimated. Nevertheless, the trend shown in Table 1 is consistent with that demonstrated by the UV−visible spectrometric (vide supra) and QCM results described at the end of this paper.

The revelation of the DNA structural change and the variation in the surface densities of the DNA films intercalated in the PLL layers yielded a semiquantitative description about the dependence of DNA loading into the composite films on the solution ionic strength used for the film preparation. It is interesting to contrast films composed of flexible DNA molecules to those containing rigid polyelectrolytes in terms of the relationship between the film thickness and the amount of molecular adsorption. Generally, as revealed by several recent studies,[52,57] thicker films consisting of compact polyelectrolyte layers correspond to a greater amount of polyelectrolyte adsorption, and there is a direct correlation between these two parameters. However, for multilayered DNA/polyelectrolyte composite films, our results clearly suggest that there is really no direct correlation between the amount of DNA incorporation (adsorption) and the DNA film thickness. The number of DNA molecules is not only dependent on the molecular structure, but also on the surface density (or the packing pattern).

To resolve more unambiguously the change of DNA surface structures caused by the ionic strength, we conducted two additional experiments. In the first experiment, the poly[G]

TABLE 1: Structural Parameters and Surface Densities of the Topmost Poly[G] Molecules, the Cumulative Loading of Poly[G], and Poly[G]/PLL Mass Ratios at Different NaCl Concentrations[a]

	DNA structural parameters and quantities[b]					
NaCl concn (M)	av height (nm)	av width (nm)	av length/diameter (nm)[c]	density (molecules/cm^2)	poly[G] loading (ng)	mass ratio of poly[G]/PLL
0	2.1 ± 0.2	31.4 ± 2.2	110−185	1.3×10^{14}	178 ± 12	2.5:1
0.1	2.9 ± 0.1	55.0 ± 5.0	50−60	3.3×10^{14}		
0.5	8.0 ± 0.7	84.0 ± 6.5	75−100	4.5×10^{14}	236 ± 10	4.2:1
1.0	11.7 ± 1.3	106.0 ± 13.1	75−120[d]	1.5×10^{14}	75 ± 8	1.2:1

[a] Films containing (PLL/Poly[G])$_3$ were prepared using 150 μg/mL poly[G] solutions of different NaCl concentrations. [b] Average of at least three replicates. [c] For circular poly[G] molecules, the length and width are equivalent to the diameter. The width is averaged over all of the strands or circles, whereas the length/diameter is given as a range. [d] The shape of most of the molecules for this case is oblong.

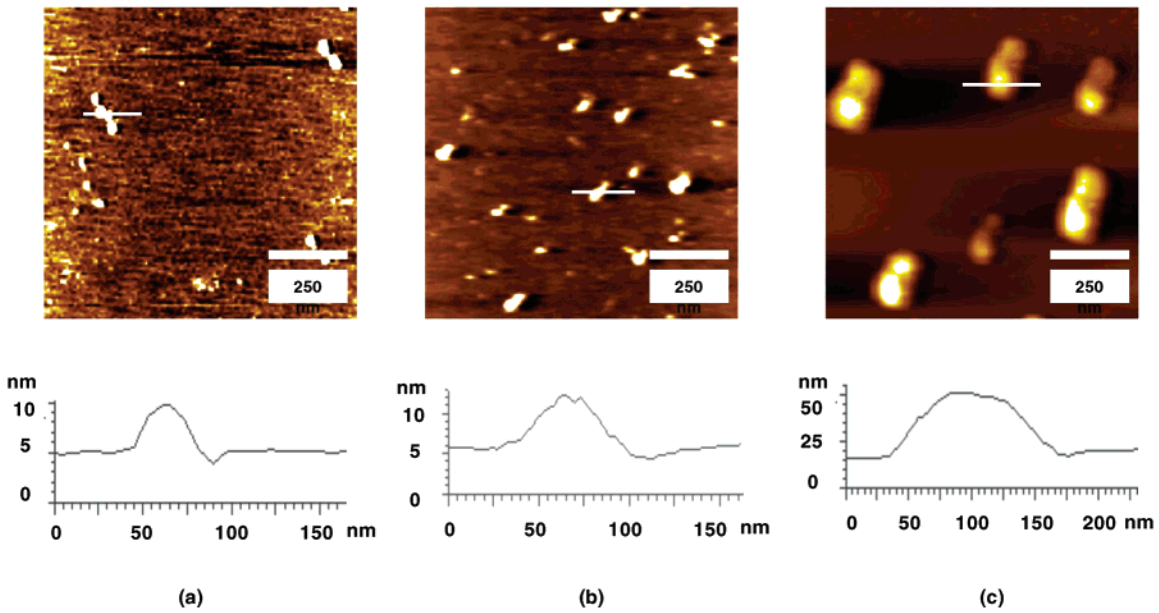

Figure 5. Topographical AFM images of poly[G] adsorbed onto APTES-treated mica surfaces. Solutions containing 3 μg/mL of poly[G] and (a) 0, (b) 0.5, and (c) 1.0 M salt were employed for the film preparation. The cross-sectional contour of each image is also provided.

concentration used in the LbL procedure was reduced to 3 μg/mL and only a single PLL/poly[G] bilayer was imaged. The effect of three representative ionic strengths (0, 0.5, and 1.0 M NaCl) on the structure and surface density of the immobilized DNA molecules was investigated. The second experiment was similar to the first, except that a positively charged mica surface was employed to mimic a PLL layer. Creation of positive charges on the mica surface was accomplished by treating a freshly cleaved mica sample with APTES.[51,58] Both experiments displayed a marked change in the poly[G] molecular shape and surface distribution. We found that the second experiment produced better-resolved images of the surface-confined DNA molecules. This is not surprising, as flat surfaces are known to give a better contrast/background for the high-quality AFM imaging of biomolecules.[54,58−62] Shown in Figure 5a−c are AFM images of three mica samples partially covered by poly-[G] molecules adsorbed from poly[G] solutions with NaCl concentrations of 0, 0.5, and 1.0 M, respectively. As can be seen in Figure 5a, several oblong DNA molecules can be clearly resolved. The use of a low poly[G] concentration prevented the immobilized DNA molecules from being interwoven. When the NaCl concentration was increased to higher NaCl concentrations (0.5 M in Figure 5b and 1.0 M in Figure 5c), similar to those in Figure 4c,d, the poly[G] molecules evolved into circular features. We should point out that the number of poly[G] molecules in a unit area is the highest in Figure 5b. This is in line with the maximum DNA loading shown in the UV−visible spectrometric measurements (Figure 3a). It is also interesting to note that the cross-sectional contours yielded a poly[G] width transition from 58.3 ± 2.9 nm (Figure 5a) to 77.9 ± 3.9 nm (Figure 5b) and finally to 166 ± 14.8 nm (Figure 5c). These values are in good agreement with those deduced from the cross-sectional contours of Figure 4a,c,d, suggesting again that the ionic strength of the DNA solution exerts a similar influence on the shape and packing of the DNA molecules onto both a positively charged solid substrate and a polyelectrolyte film.

We should add that all of the surface parameters (e.g., DNA surface coverage and structure) described above should be of equilibrium values because for a given system the attachment of each alternate adsorbate layer can be rapidly accomplished (e.g., 1−2 min for 90% adsorption of species in a dilute solution[63]) and the adsorption time employed in this work (typically 15 min) far exceeds the equilibration time. Moreover, an extensive adsorption time (e.g., several hours) was not found to cause a great extent of DNA adsorption. This implies that the attachment of DNA molecules onto the surface from a dilute solution is probably not due to diffusion-limited adsorption.

Finally, quantities of PLL and poly[G] and ratios between these quantities were gauged by QCM. For each alternate PLL and poly[G] bilayer, we found that the mass ratio between the quantity of poly[G] and that of PLL is essentially constant.

However, the ratio fluctuates among the three representative ionic strengths used. For example, when $(PLL/poly[G])_3$ was examined, the total quantity of poly[G], calculated by eq 1, over that of PLL yields 178 ± 12, 236 ± 10, and 75 ± 8 ng (Table 1) for NaCl concentrations of 0, 0.5, and 1.0 M, respectively. Despite the fact that the accuracy of QCM measurements of DNA adsorption is known to be prone to the uncertainty associated with viscoelastic effects,[64] particularly for cases when the adsorbed DNA molecules are hydrated and their strands extend beyond the effective acoustic envelop of the QCM crystal,[65] the variation of the PLL/poly[G] mass ratio appears to reflect, qualitatively or semiquantitatively, the influence of the DNA surface structure on the extent of PLL adsorption. Moreover, as seen from Table 1, films prepared using 0.5 M NaCl yielded the highest mass ratio of PLL/poly[G], which is consistent with the UV−visible spectrometric results and AFM observations.

4. Conclusion

Films composed of alternating layers of poly-L-lysine (PLL) and DNA (either polyguanylic acid, poly[G], or an oligodeoxynucleotide of 30 bases) were constructed using the layer-by-layer method. The attachment of each PLL or DNA layer was monitored by UV−visible spectrometry and contact angle measurements, the structure and surface density of the DNA molecules were measured by atomic force microscopy, and the mass ratios between the PLL and DNA layers were determined by a quartz crystal microbalance. The total amount of DNA incorporated into the $(PLL/DNA)_n$ composite films was found to be dependent on several factors, such as the DNA concentration, the number of polyelectrolyte layers, and the electrolyte concentration in the DNA solutions. While the amount of DNA incorporation increases with the number of polyelectrolyte layers and the DNA concentration, electrolyte concentrations at very low or high levels were found both to decrease the extent of DNA incorporation into the composite film. AFM images of DNA molecules situated on top of the $(PLL/DNA)_n$ films formed at different electrolyte concentrations were collected. The structure and the surface density of the DNA molecules revealed that at low electrolyte concentrations the DNA molecules are more extended and the surface density is not as high as that of the coiled DNA molecules packed at relatively high electrolyte concentrations. At very high electrolyte concentrations (e.g., 1 M), the surface density of the DNA molecules becomes scarcer because the large number of cations in the solution begins to shield the DNA molecules from the positive charges on the PLL. As a consequence of the decrease in the electrostatic attraction between PLL and DNA, DNA molecules could not be densely attached onto the PLL surface. The elucidation about the surface structure and density of the DNA molecules in the PLL/DNA composite films prepared under different conditions helps to clarify a possible misconception about the relationship between the DNA film thickness and the amount of DNA loading. Our study concerning the effect of the experimental parameters on the extent of DNA incorporation and the structures of DNA molecules in the films forms a constructive basis for future studies regarding the attachment of multilayers of DNA onto colloidal templates for the gene therapy delivery application.

Acknowledgment. This work was supported by a NIH-SCORE Grant (GM 08101), the NSF-CRUI program (Grant No. DBI-9978806) and the NSF-CEA-CREST program at CSULA. Dr. S. Han is acknowledged for his valuable suggestions.

References and Notes

(1) Langer, R. *Science* **2001**, *293*, 58−59.
(2) Lambert, G.; Fattal, E.; Couvreur, P. *Adv. Drug Delivery Rev.* **2001**, *47*, 99−112.
(3) Howard, K. A.; Dash, P. R.; Read, M. L.; Ward, K.; Tomkins, L. M.; Nazarova, O.; Ulbrich, K.; Seymour, L. W. *Biochim. Biophys. Acta* **2000**, *1475*, 245−255.
(4) Kneuer, C.; Sameti, M.; Bakowsky, U.; Schiestel, T.; Schirra, H.; Schmidt, H.; Lehr, C. M. *Bioconjugate Chem.* **2000**, *11*, 926−932.
(5) Kneuer, C.; Sameti, M.; Haltner, E. G.; Schiestel, T.; Schirra, H.; Schmidt, H.; Lehr, C. M. *Int. J. Pharm.* **2000**, *196*, 257−261.
(6) Mao, H. Q.; Roy, K.; Troung-Le, V. L.; Janes, K. A.; Lin, K. Y.; Wang, Y.; August, J. T.; Leong, K. W. *J. Controlled Release* **2001**, *70*, 399−421.
(7) Truong-Le, V. L.; Walsh, S. M.; Schweibert, E.; Mao, H. Q.; Guggino, W. B.; August, J. T.; Leong, K. W. *Arch. Biochem. Biophys.* **1999**, *361*, 47−56.
(8) Junghans, M.; Kreuter, J.; Zimmer, A. *Biochim. Biophys. Acta* **2001**, *1544*, 177−188.
(9) Hwang, S.; Davis, M. *Curr. Opin. Mol. Ther.* **2001**, *3*, 183.
(10) Affleck, D. G. *Gene Ther.* **2001**, *8*, 349.
(11) Cohen, H.; Levy, R. J.; Gao, J.; Fishbein, I.; Kousaev, V.; Sosnowski, S.; Slomkowski, S.; Golomb, G. *Gene Ther.* **2000**, *7*, 1896−1905.
(12) Hirosue, S.; Muller, B. G.; Mulligan, R. C.; Langer, R. *J. Controlled Release* **2001**, *70*, 231−242.
(13) Maruyama, A.; Ishihara, T.; Kim, J. S.; Kim, S. W.; Akaike, T. *Bioconjugate Chem.* **1997**, *8*, 735−742.
(14) Tinsley-Brown, A. M.; Fretwell, R.; Dowsett, A. B.; Davis, S. L.; Farrar, G. H. *J. Controlled Release* **2000**, *66*, 229−241.
(15) Decher, G. *Science* **1997**, *277*, 1232.
(16) Lvov, Y.; Ariga, K.; Ichinose, I.; Kunitake, T. *J. Am. Chem. Soc.* **1995**, *117*, 6117.
(17) Onda, M.; Lvov, Y.; Ariga, K.; Kunitake, T. *Biotechnol. Bioeng.* **1996**, *51*, 163.
(18) Caruso, F.; Niikura, K.; Furlong, D. N.; Okahata, Y. *Langmuir* **1997**, *13*, 3427.
(19) Araki, K.; Wagner, M. J.; Wrighton, M. S. *Langmuir* **1996**, *12*, 5393.
(20) Yoo, D.; Wu, A. P.; Lee, J.; Rubner, M. F. *Synth. Met.* **1997**, *85*, 1425.
(21) Ariga, K.; Lvov, Y.; Kunitake, T. *J. Am. Chem. Soc.* **1997**, *119*, 2224.
(22) Lvov, Y.; Ariga, K.; Ichinose, I.; Kunitake, T. *Thin Solid Films* **1996**, *285*, 797−801.
(23) Kim, D. W.; Blumstein, A.; Tripathy, S. K. *Chem. Mater.* **2001**, *13*, 1916−1922.
(24) Kim, D. W.; Blumstein, A.; Kumar, J.; Tripathy, S. K. *Chem. Mater.* **2001**, *13*, 243−246.
(25) Mamedov, A.; Ostrander, J.; Aliev, F.; Kotov, N. A. *Langmuir* **2000**, *16*, 3941−3949.
(26) Cool, P.; Clearfield, A.; Mariagnanam, V.; Ellistrem, L. J. M.; Crooks, R. M.; Vansant, E. F. *J. Mater. Chem.* **1997**, *7*, 443−448.
(27) Keller, S. W.; Kim, H. N.; Mallouk, T. E. *J. Am. Chem. Soc.* **1994**, *116*, 8817.
(28) Kleinfeld, E. R.; Ferguson, G. S. *Science* **1994**, *265*, 370.
(29) Kotov, N. A.; Dekany, I.; Fendler, J. H. *J. Phys. Chem.* **1995**, *99*, 13065.
(30) Kotov, N. A.; Haraszti, T.; Turi, L.; Zavala, G.; Geer, R. E.; Dekany, I.; Fendler, J. H. *J. Am. Chem. Soc.* **1997**, *119*, 6821.
(31) Schmitt, J.; Decher, G.; Dressick, W. J.; Brandow, S. L.; Geer, R. E.; Shashidhar, R.; Calvert, J. M. *Adv. Mater.* **1997**, *9*, 61.
(32) Feldheim, D. L.; Grabar, K. C.; Natan, M. J.; Mallouk, T. E. *J. Am. Chem. Soc.* **1996**, *118*, 7640.
(33) Lvov, Y.; Ariga, K.; Onda, M.; Ichinose, I.; Kunitake, T. *Langmuir* **1997**, *13*, 6195.
(34) Liu, Y. J.; Wang, Y. X.; Claus, R. O. *Chem. Phys. Lett.* **1998**, *298*, 315−319.
(35) Fendler, J. H. *Chem. Mater.* **1996**, *8*, 1616−1624.
(36) Caruso, F.; Rodda, E.; Furlong, D. F.; Niikura, K.; Okahata, Y. *Anal. Chem.* **1997**, *69*, 2043−2049.
(37) Lvov, Y.; Decher, G.; Sukhorukov, G. *Macromolecules* **1993**, *26*, 5396−5399.
(38) Sukhorukov, G. B.; Möhwald, H.; Decher, G.; Lvov, Y. M. *Thin Solid Films* **1996**, *284*−*285*, 220−223.
(39) Decher, G.; Lehr, B.; Lowack, K.; Lvov, Y.; Schmitt, J. *Biosens. Bioelectron.* **1994**, *9*, 677.
(40) Zhou, X. C.; Huang, L. Q.; Li, S. F. Y. *Biosens. Bioelectron.* **2001**, *16*, 85−95.
(41) Pei, R. J.; Cui, X. Q.; Yang, X. R.; Wang, E. K. *Chin. J. Chem.* **2001**, *19*, 433−435.
(42) Lang, J.; Liu, M. *J. Phys. Chem. B* **1999**, *103*, 11393−11397.

(43) Liu, M. H.; Yamashita, K. *Sci. China, Ser. B* **1999**, *42*, 567−570.
(44) Wang, J.; Rivas, G.; Luo, D.; Cai, X.; Vaiera, F. S.; Dontha, N. *Anal. Chem.* **1996**, *68*, 4365−4369.
(45) Dudnik, V.; Sukhorukov, G. B.; Radtchenko, I. L.; Möhwald, H. *Macromolecules* **2001**, *34*, 2329−2334.
(46) Trubetskoy, V. S.; Loomis, A.; Hagstrom, J. E.; Budker, V. G.; Wolff, J. A. *Nucleic Acids Res.* **1999**, *27*, 3090−3095.
(47) Lehninger, A. L.; Nelson, D. L.; Cox, M. M. *Principles of Biochemistry*; Worth Publishers: New York, 1993.
(48) Tedeschi, C.; Caruso, F.; Mowald, H.; Kirstein, S. *J. Am. Chem. Soc.* **2000**, *122*, 5841.
(49) Kern, W. *Semicond. Int.* **1984**, 94.
(50) Sauerbrey, G. *Z. Phys.* **1959**, *155*, 206.
(51) Huang, E.; Zhou, F.; Deng, L. *Langmuir* **2000**, *16*, 3272−3280.
(52) McAloney, R. A.; Sinyor, M.; Dudnik, V.; Goh, M. C. *Langmuir* **2001**, *17*, 6655−6663.
(53) Maruyama, A.; Ishihara, T.; Kim, J. S.; Kim, W. S.; Akaike, T. *Colloids Surf., A* **1999**, *153*, 439−443.
(54) Li, J.; Bai, C.; Wang, C.; Zhu, C.; Lin, Z.; Li, Q.; Cao, E. *Nucleic Acids Res.* **1998**, *26*, 4785−4786.
(55) Bustamante, C.; Keller, D.; Yang, G. *Curr. Opin. Struct. Biol.* **1993**, *3*, 363−372.
(56) Kossek, S.; Padste, C.; Tiefenauer, L. X. *Biosens. Bioelectron.* **1998**, *13*, 31−48.
(57) Dubas, S. T.; Schlenoff, J. B. *Langmuir* **2001**, *17*, 7725−7727.
(58) Hu, J.; Wang, M.; Weier, H. U. G.; Frantz, P.; Kolbe, W.; Ogletree, D. F.; Salmeron, M. *Langmuir* **1996**, *12*, 1697−1700.
(59) Huang, E.; Satjapipat, M.; Han, S.; Zhou, F. *Langmuir* **2001**, *17*, 1215−1224.
(60) Hansma, H. G.; Revenko, I.; Kim, K.; Laney, D. E. *Nucleic Acids Res.* **1996**, *24*, 713−720.
(61) Bustamante, C.; Keller, D.; Yang, G. *Curr. Opin. Struct. Biol.* **1993**, *3*, 363−372.
(62) Hansma, H. G.; Golan, R.; Hsieh, W.; Lollo, C. P.; Mullen-Ley, P.; Kwoh, D. *Nucleic Acids Res.* **1998**, *26*, 2481−2487.
(63) Schüler, C.; Caruso, F. *Biomacromolecules* **2001**, *2*, 921−926.
(64) Cavic, B. A.; Hayward, G. L.; Thompson, M. *Analyst* **1999**, *124*, 1405.
(65) Fawcett, N. C.; Craven, R. D.; Zhang, P.; Evans, J. A. *Anal. Chem.* **1998**, *70*, 2876−2880.